https://doi.org/10.15407/knit2024.02.015
UDC 621.45

O. ABADA, Professor
E-mail: abadaomar@ymail.com
H. KBAB, Professor
E-mail : k71hakim@gmail.com
S. HAIF, Doctoral degree
ORCID 0000-0002-9810-761X
E-mail : haif.sidali@etu.univ-blida.dz
Aeronautical Sciences Laboratory (LSA)
Aeronautics and Space Studies Institute
Blida 1 University BP270 Soumaa street, Blida, Algeria

OPTIMIZING THE DESIGN OF A SUPERSONIC PLANAR DUAL BELL NOZZLE

Dual bell nozzles present a promising solution for maximizing propulsion efficiency at high altitudes, while also mitigating dangerous side loads at lower altitudes. Such nozzles are comprised of two distinct contours, with the first optimized for low altitude operation, and the second tailored for high altitude conditions. These contours are interconnected at an inflexion point. The present study focuses on optimizing the contour design of a planar dual bell nozzle. Leveraging the commercial ANSYS-Fluent software, we conducted an investigation into the influence of the inflection angle on the transition between the two operating modes, examined the flow behavior inside the nozzle, and assessed the impact of the inflection angle on the thrust coefficient.

Keywords: *dual bell nozzles, the inflection angle, optimization.*

1. INTRODUCTION

When it comes to supersonic nozzles and altitude, there are indeed adaptation issues related to changes in atmospheric pressure at different altitudes. Nozzles are devices designed to optimize the efficiency of jet engines by converting the energy of gases into propulsion. Supersonic jet engines typically use convergent-divergent nozzles, also known as De Laval nozzles, to achieve supersonic exhaust velocities [2].

At low altitudes, where atmospheric pressure is high, convergent-divergent nozzles work well in accelerating the exhaust gases to supersonic speeds [8]. However, as altitude increases, atmospheric pressure decreases, which can lead to adaptation problems.

At high altitudes, the low atmospheric pressure reduces the confinement pressure inside the nozzle, which can result in excessive expansion of the exhaust gases. This can cause efficiency losses and a decrease in thrust. The excessive expansion can also lead to operational instabilities, such as nozzle flow separation, where the gas flows are no longer attached to the internal walls of the nozzle, resulting in thrust loss and propulsion instability [3, 11].

Цитування: Abada O., Kbab H., Haif S. Optimizing the Design of a Supersonic Planar Dual Bell Nozzle. *Space Science and Technology.* 2024. **30**, № 2 (147). P. 15—27. https://doi.org/10.15407/knit2024.02.015

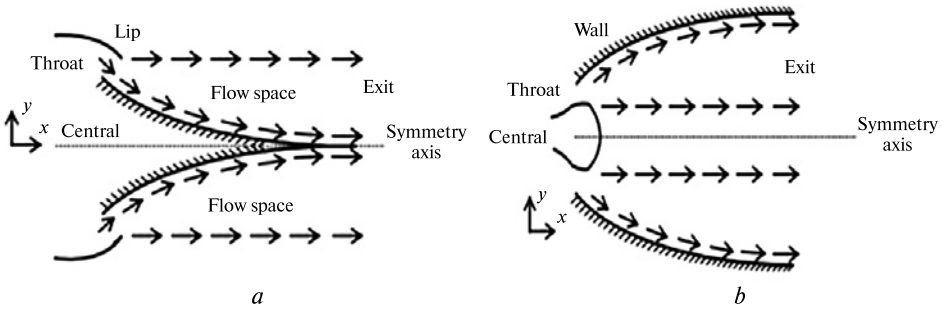

Figure 1. Nozzle geometry: *a* — plug nozzle, *b* — E-D nozzle

To overcome these adaptation issues, some supersonic nozzles are designed with variable geometry adjustment systems, such as variable geometry nozzles [4].

The dual bell nozzle is one such design that utilizes nozzle wall inflection to achieve altitude adaptation. At low altitudes, the dual bell nozzle achieves a controlled and symmetrical separation of flow at the wall inflection, resulting in a less effective expansion ratio. As the altitude increases, the flow remains attached to the nozzle wall until the full geometrical expansion ratio is utilized. This design allows for better performance and efficiency across different altitudes, addressing the challenges faced by fixed geometry nozzles. In 1949, Cowles and Foster first introduced the concept of a dual bell nozzle, and the design was patented by Rocketdyne in the 1960s [1, 6, 10]. Many researchers have been interested in the study of these nozzles. These studies have focused on contour design [5, 16]. Among these studies, there are experimental studies [17, 18] and numerical studies [7, 13].

Another type of nozzle that addresses altitude compensation is the expansion-deflection (E-D) nozzle. This nozzle achieves altitude compensation through the interaction of exhaust gas with the surrounding atmosphere [15]. The E-D nozzle controls its area ratio based on the ambient pressure, allowing it to achieve altitude compensation up to the design pressure [14]. This feature ensures that the nozzle performs optimally across different altitudes by adjusting the expansion area according to the surrounding atmospheric conditions, enhancing overall rocket performance and efficiency.

In summary, the problem of adapting supersonic nozzles with altitude lies in the need to optimize the nozzle geometry to maintain efficient and stable performance at different altitudes. Jet engine designers are working on solutions such as variable geometry nozzles to overcome these challenges.

The present study focuses on optimizing the contour design of a planar dual bell nozzle (PDBN). Leveraging the commercial ANSYS-Fluent software, we conducted an investigation into the influence of the inflection angle on the transition between the two operating modes, examined the flow behavior inside the nozzle, and assessed the impact of the thrust coefficient (Cf).

2. METHODOLOGY

This section aims to describe the method employed in designing the PDBN, which is carried out in two parts.

1. ***Design of the first contour***. The first divergent is a contour of an E-D supersonic nozzle that gives uniform parallel flow at the exit. For the design of the first nozzle profile, we have developed a program in FORTRAN. This program is inspired by the program that designs the contour of the Plug nozzle [19] with changes in parameters and principle (see Fig. 1). The design method is based on the function of Prandtl Meyer.

$$\nu(M)=\left(\frac{\gamma+1}{\gamma-1}\right)^{\frac{1}{2}}\tan^{-1}\left[\frac{\gamma-1}{\gamma+1}\left(M^2-1\right)\right]^{\frac{1}{2}}- \\ -\tan^{-1}\left(M^2-1\right)^{\frac{1}{2}}. \quad (1)$$

The number of Mach $M=1.00$ at the throat and it accelerates to the Mach number M_E at the exit section. ν is the angle between the velocity vector of the

throat and the x-axis. The lines shown in Fig. 2 represent the Mach waves, they are inclined with angle u (Angle of Mach), and the flow properties are constant along each line of Mach exits from point A.

Between the line AB and AE, there is an infinity of Mach waves, exit of point A, centered. Each line gives a Mach number, from these lines which we can easily deduct a point on the wall (the flow properties are constant along each line of Mach). As the gas is perfect, the velocity vector is tangent with a stream line, which will be regarded as the contour of Plug wall to require (The main idea of this method). To have a Mach number required at the exit, the flow to the throat must be tilted at an angle θ_B (Flow deviation compared to the horizontal).

$$\theta_B = \nu\left(M_E\right). \quad (2)$$

Figure 3 presents the parameters of an intermediate Mach line connecting the point A and point *i*. The determination of wall points is made explicitly.

The lines are iso-Mach curves, so the number of Mach in the center of expansion A equals also the number of Mach on the wall. The number of Mach in point *i* is given by:

$$M_i = 1 + (i-1)\left[\left(M_E - 1\right)/\left(N-1\right)\right] \left(i = 1,2,3,\ldots,N\right), \quad (3)$$

where N is the selected point number.

Once the number of Mach M_i in point *i* is known. In this case we can write:

$$u_i = \sin^{-1}\left(\frac{1}{M_i}\right), \quad (4)$$

$$\nu_i = \nu\left(M_i\right), \quad (5)$$

$$\theta_i = \varphi_i - u_i. \quad (6)$$

And for the point i+1 we have:

$$\frac{x_{i+1}}{\lambda_B} = \left(\frac{\lambda_{i+1}}{\lambda_B}\right)\cos\varphi_{i+1}, \quad (7)$$

$$\frac{y_{i+1}}{\lambda_B} = \left(\frac{\lambda_{i+1}}{\lambda_B}\right)\sin\varphi_{i+1}, \quad (8)$$

λ is the polar ray of a Mach wave with:

$$\frac{\lambda_{i+1}}{\lambda_B} = \left(\frac{\lambda_i}{\lambda_B}\right)\frac{\sin\alpha}{\sin\beta}, \quad (9)$$

$$\alpha = \pi - \varphi_i + \nu_E - \nu_i, \quad (10)$$

$$\beta = \varphi_{i+1} - \nu_E + \nu_i, \quad (11)$$

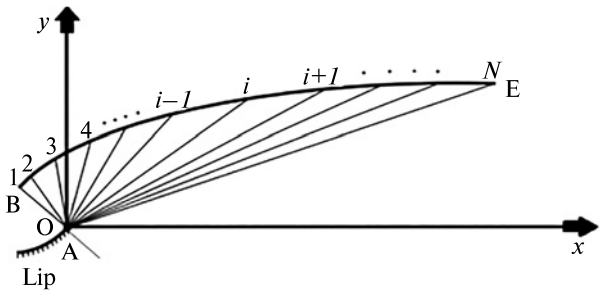

Figure 2. Discretization of the expansion zone

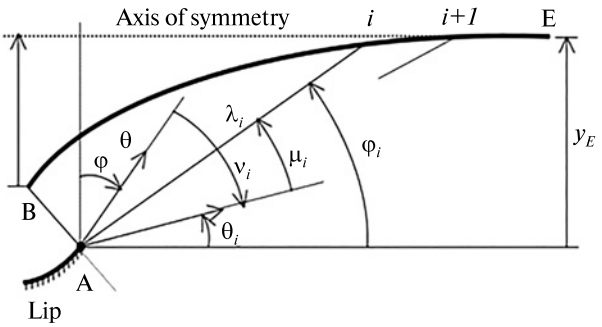

Figure 3. Parameters of an intermediate Mach

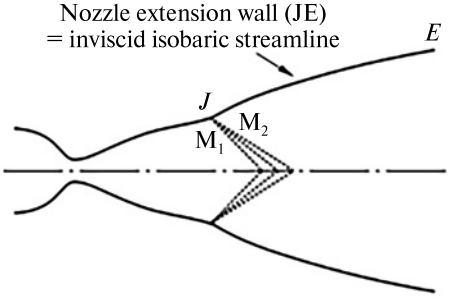

Figure 4. Centered expansion at junction J [12]

α and β (angles respectively at tops A and *i* of the triangle connecting the points *A*, *i* and *i*+1 of the Fig. 3). φ is the polar angle of Mach.

2. Design of the second contour. The contour of the nozzle extension (second bell) is designed to give a constant wall Mach number M_2. This is done by applying the characteristics method to the Prandtl-Meyer expansion around junction point *J* with equal intensity M_2/M_1 (see Fig. 4) for the inviscid fluid hypothesis.

3. INVISCID CALCULATIONS

In this study, we performed inviscid calculations to analyze the flow through the nozzle. The simulation aims to study the flow in a specific nozzle, shown in Figure 5, *a*. This figure illustrates the profile of the type E-D nozzle, with a radius of 0.6 cm and an exit area of 0.0218 m². The geometry of the nozzle was produced using our computer code developed in FORTRAN. *Y** represent throat radius. Figure 5, *b* represent the evolution of the Mach number along the wall of the E-D nozzle. It is noted that the flow increases from $M = 1.0$ in the col until $M =$ design Mach. Figure 5, *c* show the wall pressure ratio comparison between the numerical method (FORTRAN) and the simulation (ANSYS-Fluent). The results show a good similarity.

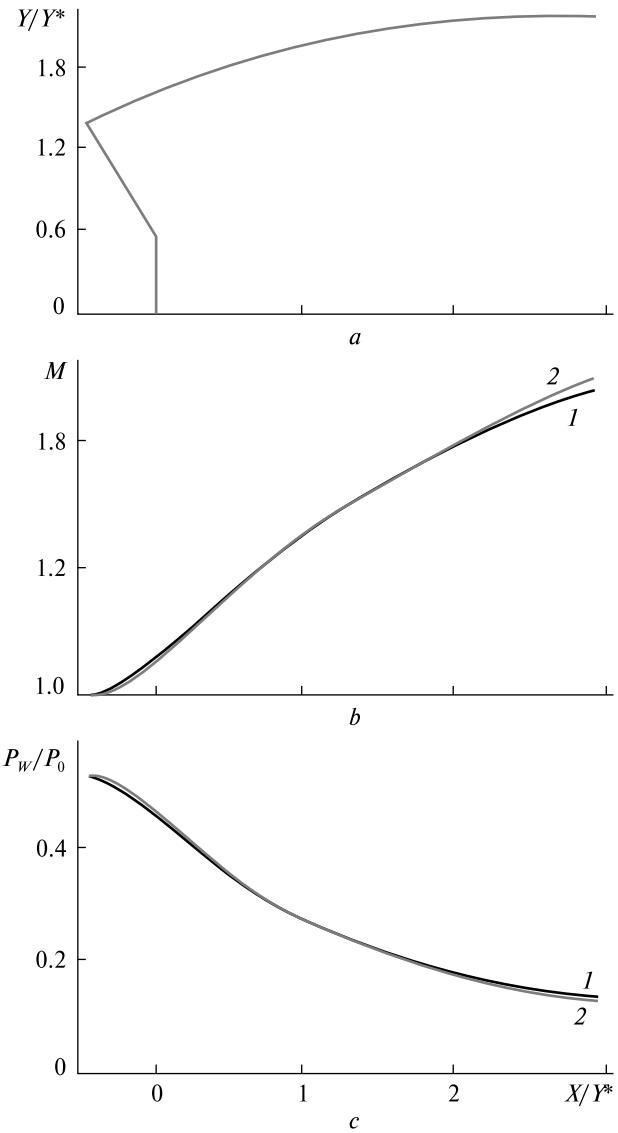

Figure 5. Profile of the E-D nozzle for Mach = 2.00 (*a*), wall Mach number evolution (*b*), wall pressure ratio evolution (*c*): *1* — ANSYS-fluent, *2* — FORTRAN

Figure 6, *a* shows the Iso-Mach contours for an E-D nozzle that works in the design Mach number obtained by our simulation. We note that in the divergent part, the number of Mach increases until reaching the value of the nozzle designing Mach number at the exit. We notice that the number of Mach at the exit of E-D nozzle is $M = 1.9$. Figure 6, *b* shows the Iso-pressure ratio contours for an E-D nozzle that works in the design Mach number obtained by our simulation. The figure shows the Prandtl — Meyer expansion fan around the lip. In addition, there are no pressure fluctuations or turbulence corresponding to a typical flow along the nozzle.

4. VISCOUS CALCULATIONS

In this part, a numerical analysis is performed on the flow through E-D nozzle. Flow analysis is performed. Numerical analysis is performed on 2D planar models using the commercial ANSYS-Fluent software. The k-ω SST model was used as the turbulence model. The baseline solver was selected as a double-precision density-based coupled solver with Implicit Time Integration. Least-square cell-based gradient is used for spatial discretization in which the solution was assumed to vary linearly was used and a second-order upwind scheme was used for interpolating the values of pressure, momentum, turbulent kinetic energy, specific dissipation rate and energy. The computational analysis was conducted under steady conditions. The initialization for steady-state problem was done using full multigrid (FMG) initialization to get the initial solution, and the inlet boundary was provided to give the reference value. Sutherland equation is used for calculating the viscosity of air. Figure 7 represent the evolution of the Iso-Mach of the E-D nozzle for different nozzle pressure ratio (NPR = 10, 36.7 and 50). For NPR = =10 (overexpansion), it is noted that the flow remains attached to the walls of the E-D nozzle.

To study the interaction of the flow of the E-D nozzle with the ambient outside, we made a com-

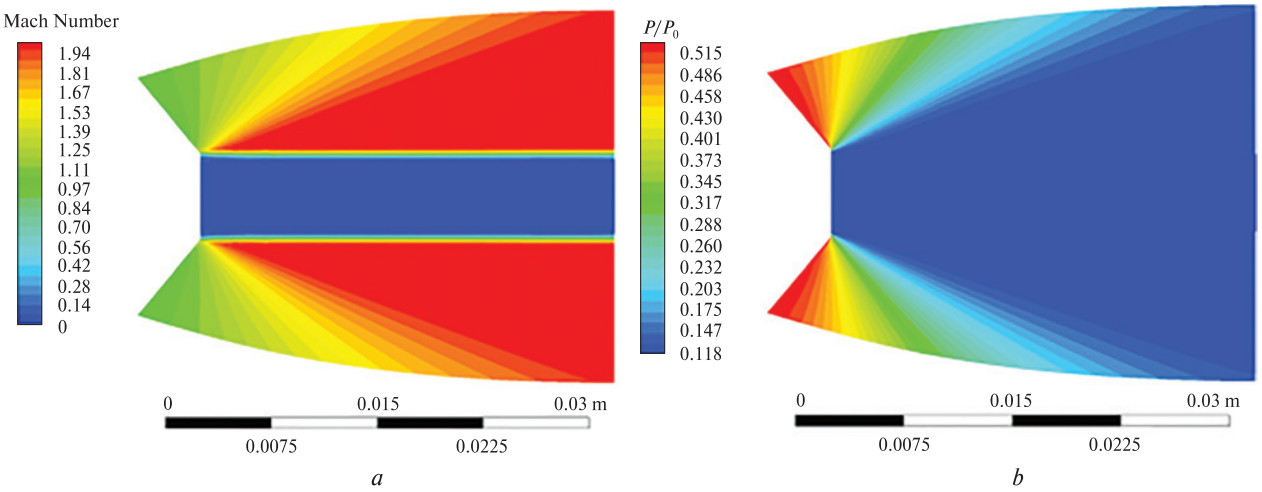

Figure 6. Iso-Mach contours (*a*) and iso-pressure ratio contours (*b*)

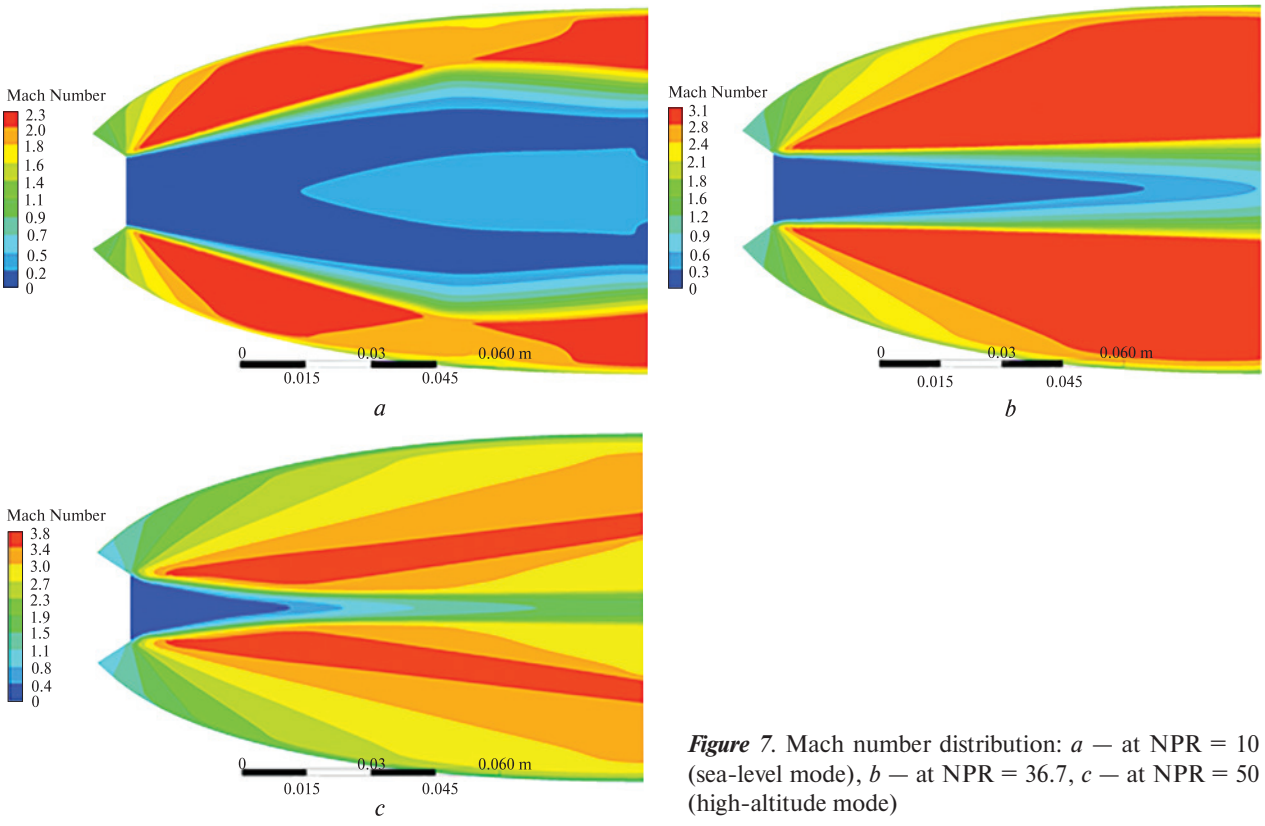

Figure 7. Mach number distribution: *a* — at NPR = 10 (sea-level mode), *b* — at NPR = 36.7, *c* — at NPR = 50 (high-altitude mode)

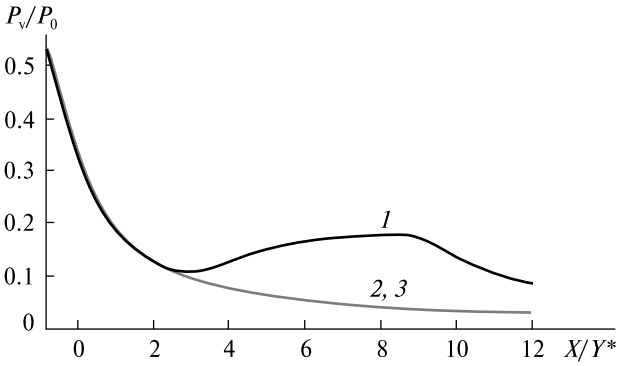

Figure 8. Wall pressure ratio distribution for different values of NPR (*1, 2, 3* — at NPR = 10, 36.7, 50 respectively)

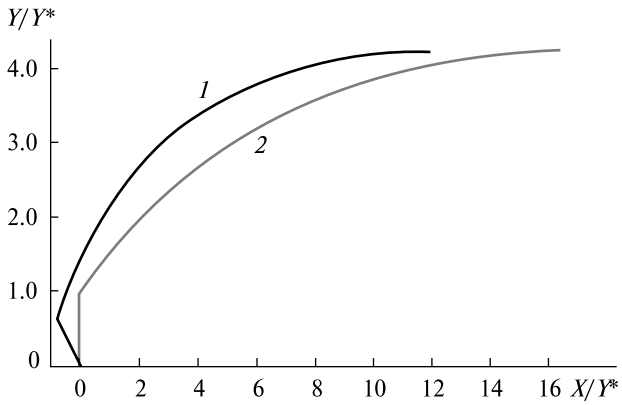

Figure 9. E-D (*1*) and CN (*2*) nozzle profile

Table 1. **Boundary conditions values**

Parameter	E-D and CN
Total pressure, Pa	200000
Static pressure, Pa	105656
Ambient pressure, Pa	26666.66 and 5000
Design Mach Number	3.0

Table 2. **Thrust of the two nozzles (CN and E-D)**

NPR	CN	E-D	Thrust gain (%)
07.0	1779.502	1995.667	10.83
40.0	2871.406	2879.632	00.29

parison of the pressure of the wall for different modes of operation (NPR). Figure 8 represents the pressure distribution on the walls of the nozzle for different pressure ratio (NPR = 10, 36.7 and 50). For NPR = 36.7 and 50 we notice that the pressure on the walls is not affected by the external environment. The main property of an E-D nozzle is its interaction with the outside environment allowing it to eliminate flow separation.

5. COMPARISON BETWEEN E-D AND CN

A flow analysis is conducted on the E-D nozzle using numerical methods. To validate the performance of this nozzle, we compare it with a conventional nozzle (CN) under similar boundary conditions (Table 1). The contour of the conventional nozzle is generated by the method of characteristic [9]. The study involves 2D planar models analyzed using the ANSYS-Fluent software, and the simulation employs the Fluent solver to solve the Reynolds-averaged Navier-Stokes equations with a k-ω SST turbulence model.

After comparing the profiles of the E-D nozzle and CN (shown in Fig. 9), it is observed that the length of the E-D nozzle is 11.97717 units, while the length of the CN is 4.2293 units, both having the same section ratio $A_e / A_t = 4.234$. This indicates a decrease in length of 27.12 % for the E-D nozzle compared to the CN. Consequently, the E-D nozzle offers a more streamlined design, leading to greater fuel savings for the E-D. In this context, A_t and A_e represent the throat area and exit area of the nozzle, respectively.

Figure 10 represent the evolution of the Iso-Mach of the E-D nozzle and CN for NPR = 7.5 and 40.0. For NPR = 7.5 (overexpansion), it is noted that the flow remains attached to the walls of the E-D nozzle, unlike the conventional nozzle in which there is a separation of the flow in the walls. This leads to the appearance of the side loads, which in turn reduces the efficiency of the nozzle.

The E-D's nozzle operates without the need for controlled flow separation mechanisms, enabling it to adapt to different altitudes. In the open wake mode (Fig. 10, *a*), the nozzle's exit region is regulated by the ambient pressure, which results in the exhaust gas not completely filling the nozzle. However, in the closed wake mode (Fig. 10, *c*), the entire exit area of the nozzle is filled by the exhaust gases. The transition

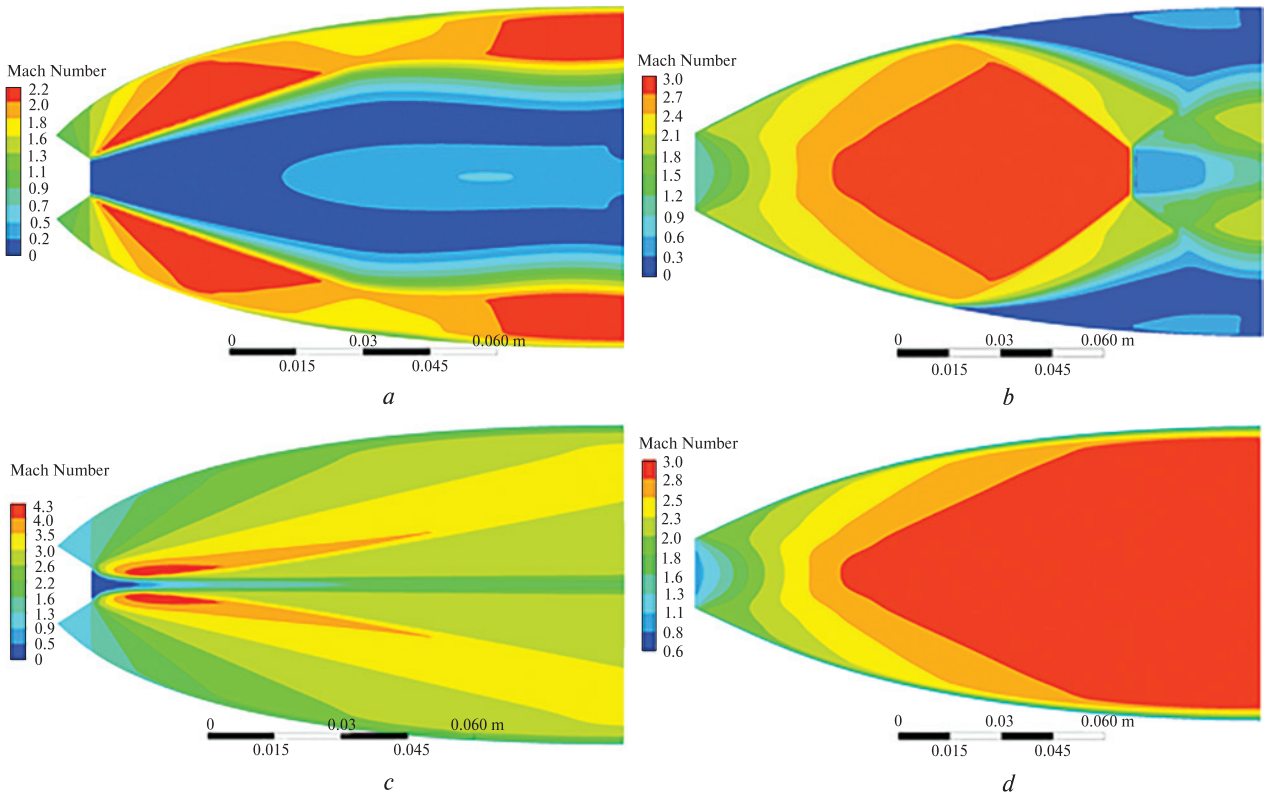

Figure 10. Iso-Mach E-D nozzle for NPR = 7.5 (*a*), iso-Mach CN nozzle for NPR = 7.5 (*b*), iso-Mach E-D nozzle for NPR = = 40 (*c*), iso-Mach C nozzle for NPR = 40 (*d*)

from the open to closed wake modes occurs at a specific ambient pressure known as the design pressure. If the ambient pressure is further decreased beyond this design pressure, the remaining expansion would occur outside the nozzle, resembling the behavior of a bell nozzle. In such a scenario, the altitude compensation benefits of the E-D's nozzle would not be applicable.

The note highlights the thrust characteristics of the E-D nozzle compared to the conventional nozzle at different pressure ratios (Table 2). When NPR is equal to 7.5, the E-D nozzle demonstrates a considerable increase in thrust compared to the conventional nozzle. At NPR 40, both the E-D nozzle and the conventional nozzle exhibit nearly equal thrust performance. This similarity in thrust is attributed to the fact that both nozzles have the same effective section. The advantage of the E-D nozzle over the conventional nozzle lies in its ability to generate higher thrust at lower pressure ratios than the design pressure ratio. However, as the pressure ratio approaches and exceeds the design pressure ratio, the thrust advantage diminishes, eventually leading to comparable performance between the two nozzles.

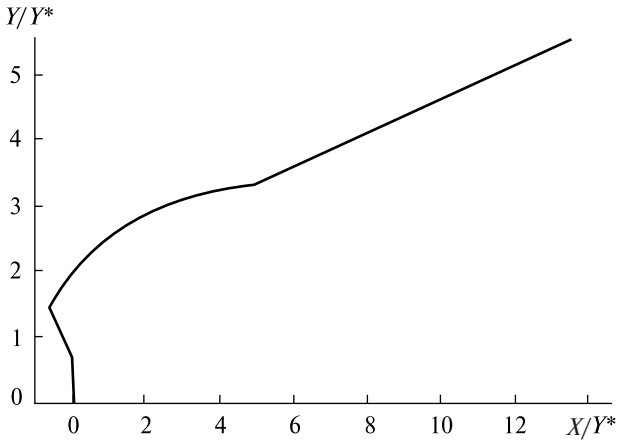

Figure 11. Planar dual bell nozzle profile

6. PLANAR DUAL BELLL NOZZLE (PDBN)

Figure 11 represents the PDBN profile obtained by our FORTRAN program. The junction point coordinates J (where the two profiles meet) are given by $X_J = 13.48$ and $Y_J = 3.31$. The total nozzle length is $L_T = 13.48$. The exit radius of the nozzle is $R_T = 5.55$.

A series of computations were initiated to investigate how the variation in nozzle pressure ratios (NPR) affects the dual bell nozzle operating mode, with particular attention to the fluid behavior near the nozzle wall. The simulations considered the NPR being linearly increased from 05.0 to 100. To accurately replicate the physics of the studied problem, the total

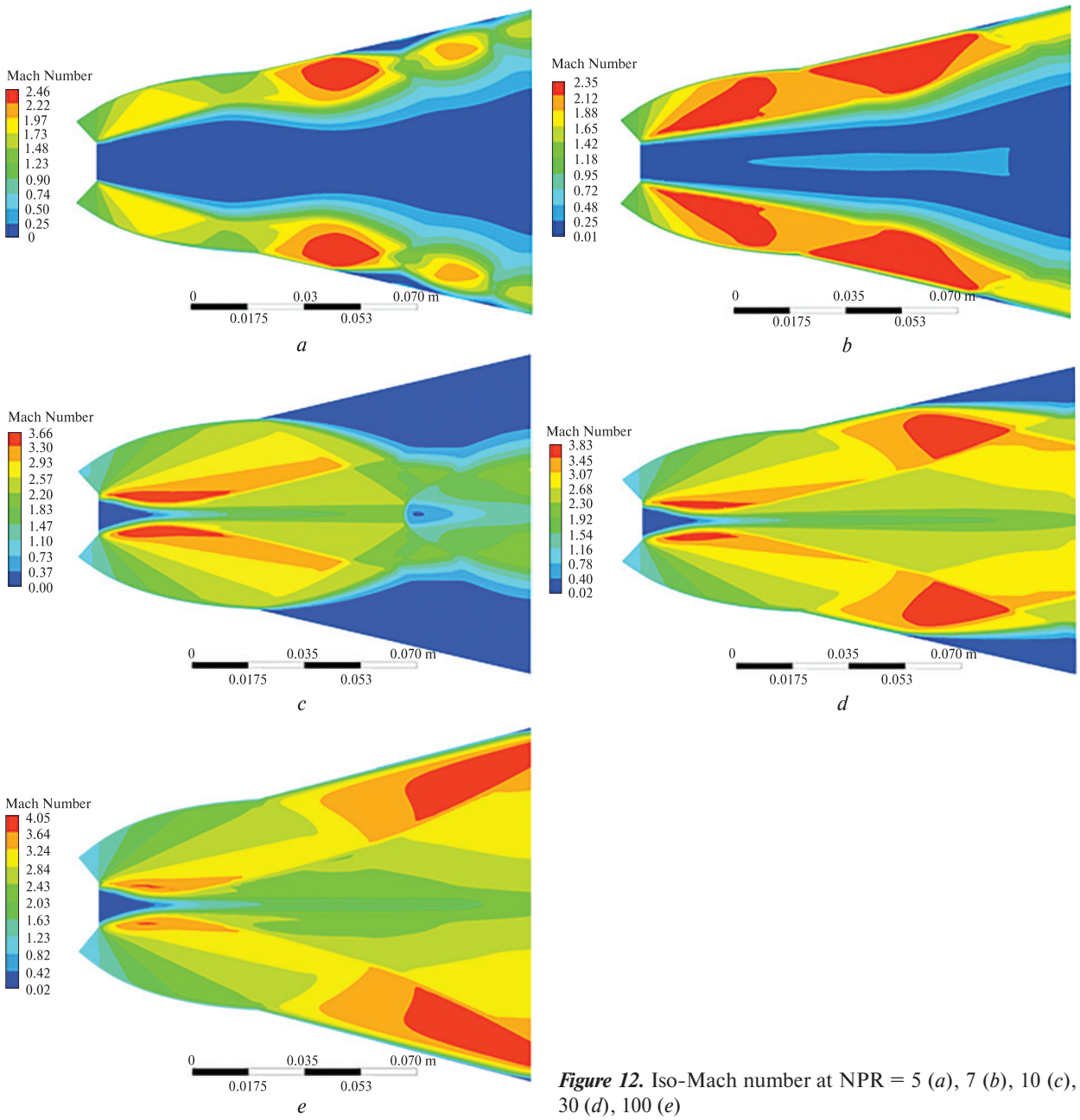

Figure 12. Iso-Mach number at NPR = 5 (*a*), 7 (*b*), 10 (*c*), 30 (*d*), 100 (*e*)

feeding pressure was maintained at a constant level, while the ambient pressure was deliberately altered. These simulations allowed us to highlight all operating modes of this nozzle while passing from sea level Mode (Fig. 12, *a*), transition Mode (Fig. 12, *d*) until the high altitude Mode (Fig. 12, *e*). The wall pressure variation according to NPR is shown in Figures 13.

For NPR = 5 and 7 the PDBN operates in the open wake mode. The flow in the second contour remains close to the wall of the nozzle, this explains the fluctuation in wall pressure ratio (curves in red and black from Fig. 13). For NPR = 10 a brutal increase in wall pressure after the inflection point. It can be seen that the separation point remains stable at the inflection point of the nozzle. This reduces the side load in low altitude mode. In the case of NPR between 10 and 90, it is noted that the separation point ramps along the extension wall of the nozzle. Consequently, the nozzle operates during this phase in transition mode. We note that for NPR = 100, the nozzle operates in high altitude mode.

In order to study the effect of geometric variables on the PDBN, and in particular on the behavior of the flow inside it, we have studied the effect of the inflection angle α (Fig. 14, *a*). Two PDBN with different inflection angle (21° and 7°) have been considered for this study. In addition to the previous PDBN (α = 14°). The inflection angle of the PDBN is varied, keeping the exit section constant. In the study of nozzle performance at various NPR (Nozzle Pressure Ratios), three different PDBN configurations, namely α = 7°, α = 14°, and α = 21°, were analyzed. The schematic diagram of 3 nozzles are provided in Fig. 14, *b*.

For NPR = 5, the PDBN with α = 7° and α = = 21° both operated in the open wake mode, similar to the PDBN with α = 14°. However, a notable contrast arose with PDBN (α = 21°), where flow separation occurred precisely at the inflection point, as depicted in Fig. 15, *a*. Upon reaching NPR = 7, the PDBN featuring α = 7° operated differently, utilizing a closed wake mode. In contrast, both PDBN with α = 14° and α = 21° remained in an open wake mode. Advancing to NPR = 10, both PDBN (α = 7° and α = 21°) operated in a closed wake mode, demonstrating their similarity in performance at this NPR. However, a significant difference became apparent at

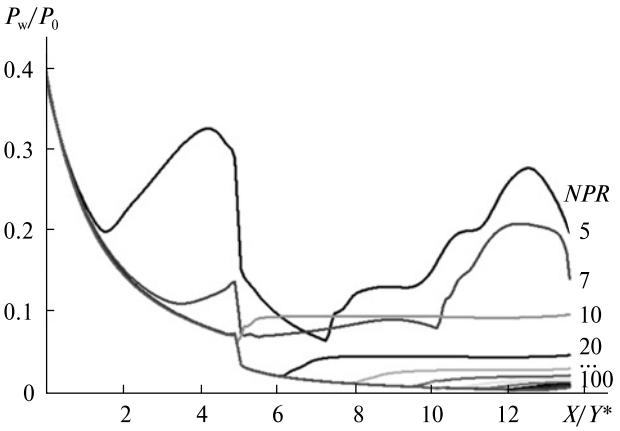

Figure 13. Wall pressure ratio distribution for different values of NPR

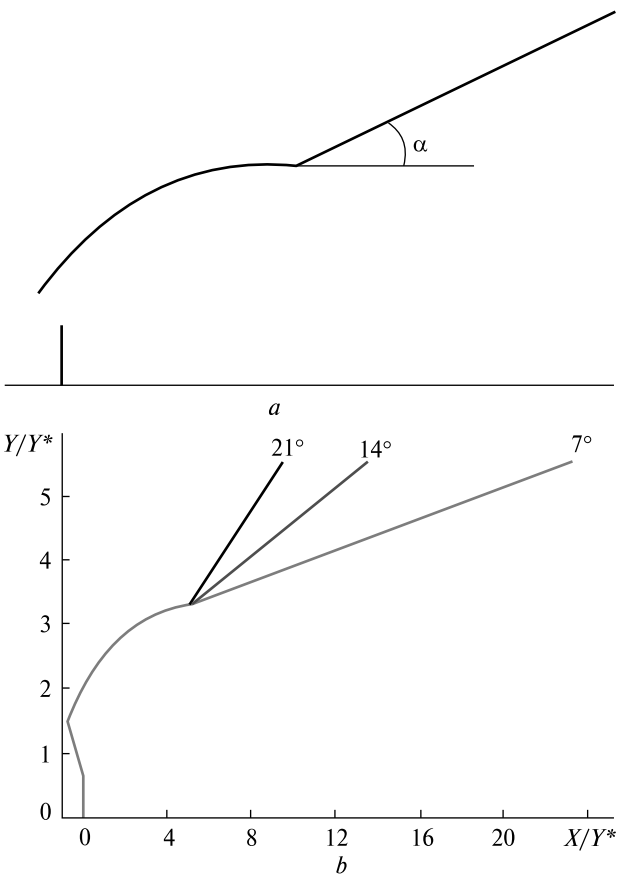

Figure 14. Schematic diagram of nozzle contour (*a*) and configuration of the 3 nozzles (*b*)

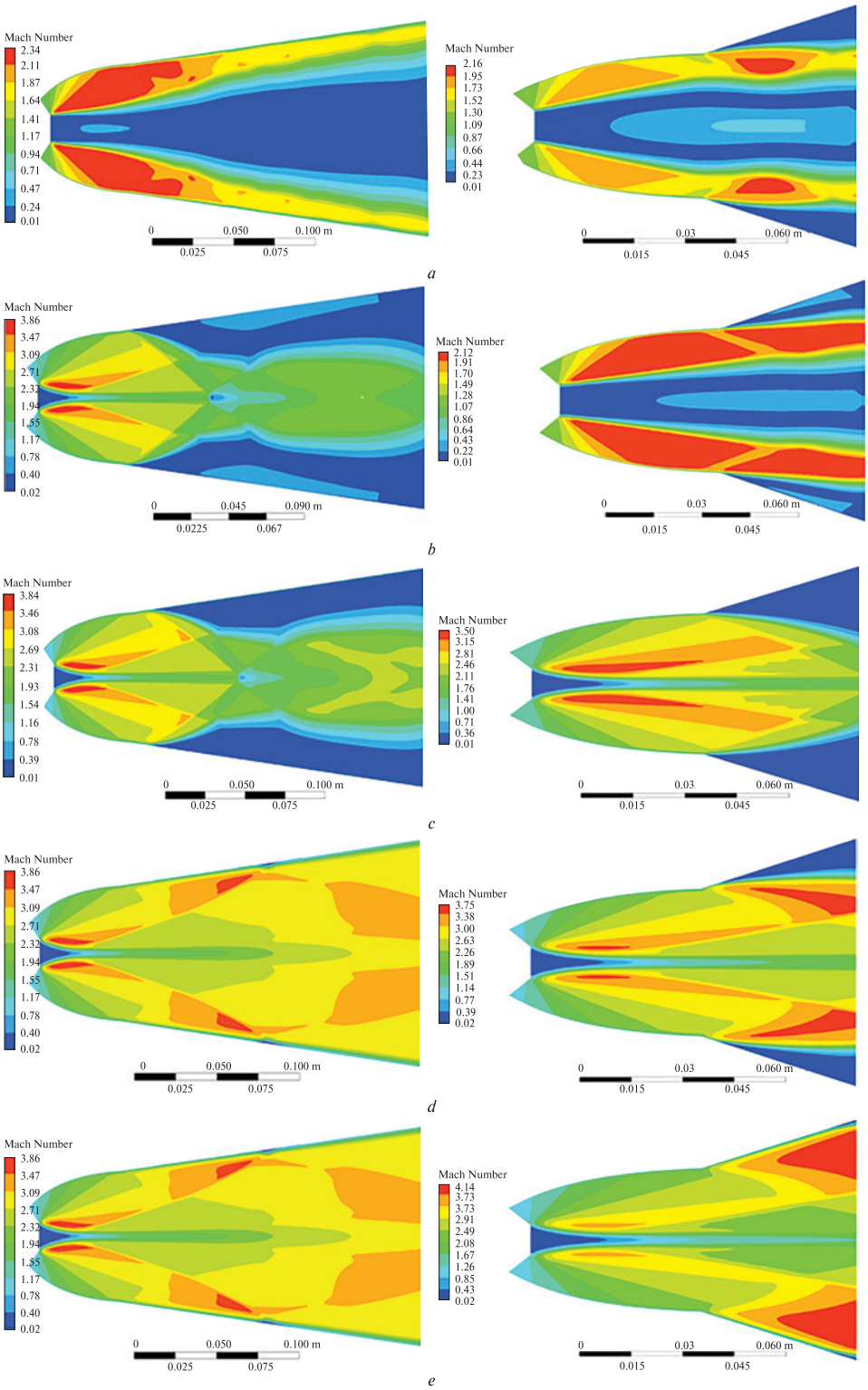

Figure 15. Iso-Mach number for α = 7° (left) and α = 21° (right) at NPR = 5 (*a*), 7 (*b*), 10 (*c*), 30 (*d*), 100 (*e*)

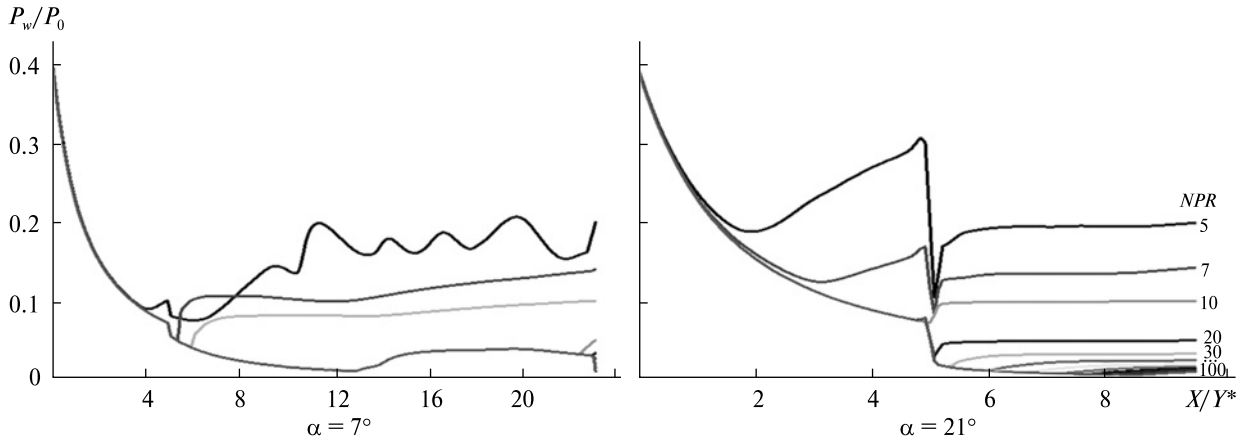

Figure 16. Wall pressure ratio distribution for different values of NPR (NPR = 5, 7, 10, 20, 30, 40, 50, 60, 70, 80, 90, 100)

NPR = 30. While flow separation was completely eliminated in the PDBN with α = 7°, the PDBN with α = 21° still experienced some separation, particularly near the inflection point. This intriguing observation occurred despite both nozzles operating at the same altitude (NPR). Finally, when reaching NPR = 100, it was found that both PDBN configurations, α = 7° and α = 21°, achieved complete elimination of flow separation, signifying their enhanced performance at higher NPR values. These findings indicate that the behavior of PDBN configurations is influenced by NPR, with certain configurations exhibiting improved flow characteristics and reduced separation at specific NPR values.

Figure 16 show Wall pressure ratio changes for different NPRs for PDBN (α = 7°) and PDBN (α = = 21°), respectively.

To investigate the impact of the inflection angle on the thrust coefficient (Cf), Fig. 17 illustrates the relationship between the two parameters for different nozzle pressure ratios (NPR). During the launch phase of the space rocket, the nozzle with a deflection angle of 21° (PDBN α = 21°) exhibits 11.19 % higher thrust compared to both PDBN α = 7° and PDBN α = 14° when NPR is set to 7°. Throughout the rest of the space flight, PDBN α = 7° demonstrates superior performance in comparison to the other nozzles. Notably, it achieves a remarkable 10.89 % increase in thrust force for NPR = 20. Additionally, PDBN α = 7° attains its maximum thrust at lower altitudes compared to the other nozzle designs.

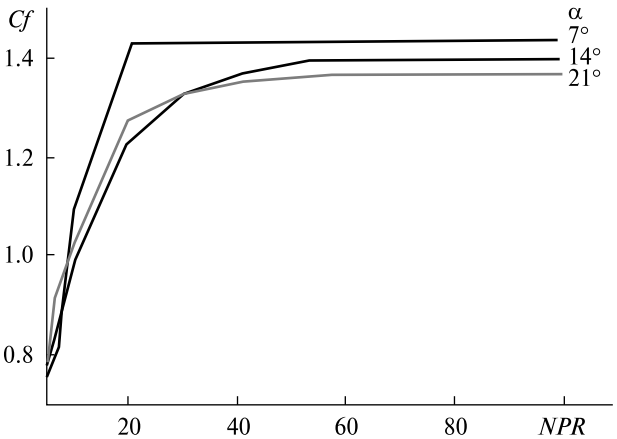

Figure 17. Comparison of thrust coefficient for different values of inflection angle

7. CONCLUSION

At the beginning of our study, we undertook an in-depth investigation of the field of propulsion nozzle design to explore the various flow behaviors through these devices. Our focus was particularly on examining two types of supersonic nozzles: the expansion-deflection nozzle and the planar dual bell nozzle (PDBN), as these configurations are still under study. The evolution of flow parameters Mach number and pressure was studied and analyzed using the simulation software ANSYS-Fluent. To carry out our study successfully, we employed a numerical simulation approach using a two-dimensional model to represent the propulsion nozzles. We assumed

a perfect gas in our calculations, allowing us to consider the primary flow characteristics.

Our study was structured into three distinct parts, each aimed at examining different aspects of propulsion nozzles based on variations in the NPR. Here is a detailed description of each of these parts:

• Simulation of the Expansion-Deflection Nozzle (E-D): In this part, we conducted simulations for both viscous and inviscid cases of the E-D nozzle. The objective was to analyze the flow characteristics through this nozzle in these two regimes. By utilizing the ANSYS-Fluent simulation code, we were able to study and compare flow behaviors, particularly in terms of Mach number, pressure, and generated thrust.

• Comparison between E-D and Convergent-Divergent Nozzles (CN): In this part, we conducted a detailed comparison between the E-D nozzles and the CN nozzles, examining parameters such as Mach number, pressure, and thrust. This comparison allowed us to gain a better understanding of the differences and relative advantages of these two types of supersonic nozzles.

• Simulation of Planar double bell Nozzle: We also focused on the PDBN and conducted simulations for a viscous flow, varying the inflection angle of the nozzle. The objective was to evaluate the impact of the geometric parameter on the performance of the PDBN and compare the obtained results.

During the design of a nozzle, it is crucial to consider the influence of the radius of the inflection angle on the flow behavior inside the nozzle. This will enable us to design a nozzle that best meets our specific performance requirements.

REFERENCES

1. Davis K., Fortner E., Heard M., McCallum H., Putzke H. (2015). Experimental and computational investigation of a dual-bell nozzle. *53rd AIAA Aerospace Sciences Meeting* (5—9 Jan., 2015, Florida).
2. Durif O. (2022). Design of de Laval nozzles for gas-phase molecular studies in uniform supersonic flow. *Phys. of Fluids*, Issue 34.
3. Hadjadj A., Onofri M. (2009). Nozzle flow separation. *Shock Waves*, Issue 19, 163—169.
4. Hagemann G., Immich H., Van Nguyen T., Dumnov G. E. (1998). Advanced rocket nozzles. *J. Propulsion and Power*, Issue 14, 620—634.
5. Hakim K., Haif S., Abada O. (2023). Design process and flow field analysis of a double divergent supersonic nozzle: Enhancing efficiency and performance. *Int. Conf. on Pioneer and Innovative Studies* (5—7 June 2023, Konya).
6. Horn M., Fisher S. (1993). Dual-bell altitude compensating nozzles. *Pennsylvania State Univ., NASA Propulsion Engineering Research Center*, **2**.
7. Kbab H., Abada O., Haif S. (2023). Numerical Investigation of Supersonic Flows on Innovative Nozzles (Dual Bell Nozzle*). J. Applied Fluid Mechanics*, Issue 16, 819—829.
8. Khan S. A., Ibrahim O. M. Aabid A. (2021). CFD analysis of compressible flows in a convergent-divergent nozzle. *Materials Today. Proceedings*, Issue 46, 2835—2842.
9. Micbael R., Goldman L. Computer program for design of two-dimensional supersonic nozzle with sharp-edged throat. *NASA TM X-1502.*
10. Nürnberger-Génin C., Stark R. (2010). Experimental study on flow transition in dual bell nozzles. *J. Propulsion and Powe*r, Issue 26, 497—502.
11. Ostlund J., Muhammad-Klingmann B. (2005). Supersonic flow separation with application to rocket engine nozzles. *Appl. Mech. Rev.*, Issue 58, 143—177.
12. Reijasse P., Coponet D., Luyssen J. M., Bar V., Palerm S., Oswald J., Kuszla P. (2011). Wall pressure and thrust of a dual bell nozzle in a cold gas facility. *Progress in Propulsion Phys.*, Issue 2, 655—674.
13. Schneider D., Génin C. (2016). Numerical investigation of flow transition behavior in cold flow dual-bell rocket nozzles. *J. Propulsion and Power*, Issue 32, 1212—1219.
14. Schomberg K. A., Doig G., Olsen J., Neely A. J. (2014). Geometric analysis of the linear expansion-deflection nozzle at highly overexpanded flow conditions. *50th AIAA/ASME/SAE/ASEE Joint Propulsion Conf.* (28—30 July, 2014, Cleveland).
15. Schomberg K., Olsen J., Neely A., Doig G. (2014). Experimental analysis of a linear expansion-deflection nozzle at highly overexpanded conditions. *19th Australasian Fluid Mechanics Conf.* (8—11 December, 2014, Melbourne).
16. Shrivastava K., Das A. K., Saha U. K. (2023). A neural network based design of a planar double divergent nozzle. *25th AIAA Int. Space Planes and Hypersonic Systems and Technologies Conf.* (May 28 — June 1, 2023, Karnataka).

17. Verma S., Hadjadj A., Haidn O. (2015). Unsteady flow conditions during dual-bell sneak transition. *J. Propulsion and Power*, Issue 31, 1175—1183.
18. Verma S., Stark R., Haidn O. (2013). Reynolds number influence on dual-bell transition phenomena. *J. Propulsion and Power*, Issue 29, 602—609.
19. Zebbiche T. (2005). Supersonic plug nozzle design. *41st AIAA/ASME/SAE/ASEE Joint Propulsion Conf. & Exhibit* (10—13 July, 2005, Arizona).

Стаття надійшла до редакції 10.10.2023 *Received 10.10.2023*
Після доопрацювання 10.012024 *Revised 10.01.2024*
Прийнято до друку 16.01.2024 *Accepted 16.01.2024*

О. Абада, проф.
E-mail: abadaomar@ymail.com
Х. Кбаб, проф.
E-mail: k71hakim@gmail.com
С. Хайф, Doctoral degree
ORCID 0000-0002-9810-761X
E-mail: haif.sidali@etu.univ-blida.dz

Aeronautical Sciences Laboratory (LSA)
Aeronautics and Space Studies Institute
Blida 1 University BP270 Soumaa street, Blida, Algeria

ОПТИМІЗАЦІЯ КОНСТРУКЦІЇ НАДЗВУКОВОГО ПЛАНАРНОГО ДВОКОНТУРНОГО СОПЛА

Двоконтурні форсунки є перспективним рішенням для максимізації ефективності руху на великих висотах, а також пом'якшення небезпечних бічних навантажень на низьких висотах. Такі форсунки складаються з двох різних контурів, причому перший оптимізовано для роботи на низькій висоті, а другий — для роботи на великій висоті. Ці контури з'єднані між собою в точці перегину. Дане дослідження зосереджено на оптимізації конструкції контуру плоского подвійного розтрубного сопла. З використанням комерційного програмного забезпечення ANSYS-Fluent досліджено вплив кута перегину на перехід між двома режимами роботи, вивчено поведінку потоку всередині сопла та оцінено вплив кута перегину на коефіцієнт тяги.

Ключові слова: двоконтурні форсунки, кут перегину, оптимізація.